J Petrol Explor Prod Technol (2017) 7:1085–1093
DOI 10.1007/s13202-016-0282-2

ORIGINAL PAPER - EXPLORATION ENGINEERING

Phase behavior of $SCCO_2$ sequestration and enhanced natural gas recovery

Yang Sun[1] · Zhimin Du[1] · Lei Sun[1] · Yi Pan[1]

Received: 15 March 2016 / Accepted: 27 August 2016 / Published online: 8 September 2016

Abstract Some noncommercial gas reservoirs with low reserves are feasible sites for CO_2 sequestration. Those gas reservoirs contain natural gas that can take up the potential pore space of $SCCO_2$ sequestration in the reservoir. The solution is to recover the natural gas by active CO_2 injection. This idea is carbon sequestration with enhancement gas recovery (CSEGR). In CSEGR, different zones of the formation fluid are formed during the gas migration. In this paper, the sequestration site is a PY gas reservoir. The pressure, volume and temperature properties of the formation fluid are tested by experiments or calculated by the program based on PR-EOS, using a *Z*-factor, Volume ratio in place ($V_{\mathrm{r.scco_2}}$), density and viscosity. We discuss those experimental or simulation results to understand the fluid phase behavior in such a migration during CSEGR in a PY gas reservoir, and we give the suitable site (temperature) and the eligible pressure of the next core-flooding test.

Keywords CSEGR · Phase behavior · $SCCO_2$ zone · $SCCO_2$–natural gas transitional zone · Natural gas zone · Gas migration

Introduction

Some noncommercial gas reservoirs with low gas reserves are feasible sites for CO_2 geological sequestration. Many of them contain natural gas that can be potentially recovered. CO_2 sequestration in those natural gas reservoirs can be coupled with enhanced gas recovery by injecting CO_2. The added gas recovery can be used to offset the cost of CO_2 capture and storage (CCS). This idea was first planned for abandoned gas reservoirs and called carbon sequestration with enhanced gas recovery (CSEGR) (Oldenburg 2003). In reality, typical noncommercial gas reservoirs are similar. Although CSEGR has been discussed for more than 10 years (for example, Blok et al. 1997), the published field tests are only in Hungary (Kubus 2010), the Netherlands (Van der Meer et al. 2005) and the USA (Turta et al. 2008).

As estimated in the Joule II Non-nuclear Energy Research Program, for maximum storage capacity, CO_2 has to be stored as supercritical CO_2 ($SCCO_2$). Published basic research on CSEGR simplifies real natural gas as pure CH_4 (Mamora and Seo 2002; Seo and Mamora 2003; Oldenburg 2003; Nogueira and Mamora 2005; Turta et al. 2008). Such research suggests that $SCCO_2$ and natural gas should not completely mix in the reservoir during the gas migration. However, the mix is multi-contact and creates the $SCCO_2$–natural gas transitional zone. Thus, the formation fluid in the whole reservoir size could be simply divided into three zones on the swept region. Such areas are the $SCCO_2$ zone, $SCCO_2$–natural gas transitional zone and natural gas zone (Figs. 1, 2). In this paper, the region connecting the $SCCO_2$–natural gas transitional zone and the natural gas zone is called the "displacement front." In addition, the region connecting the $SCCO_2$ zone and the $SCCO_2$–natural gas transitional zone is called the "storage front," both of which are shown in Figs. 1 and 2.

✉ Yang Sun
sakyana@126.com

Zhimin Du
duzhimin@swpu.edu.cn

Lei Sun
sunleiswpi@163.com

Yi Pan
panyi-1981@126.com

[1] The State Key Laboratory of Oil and Gas Reservoir Geology and Exploitation Engineering, Southwest Petroleum University, Xindu Avenue 8#, Xindu District, Chengdu 610500, Sichuan, People's Republic of China

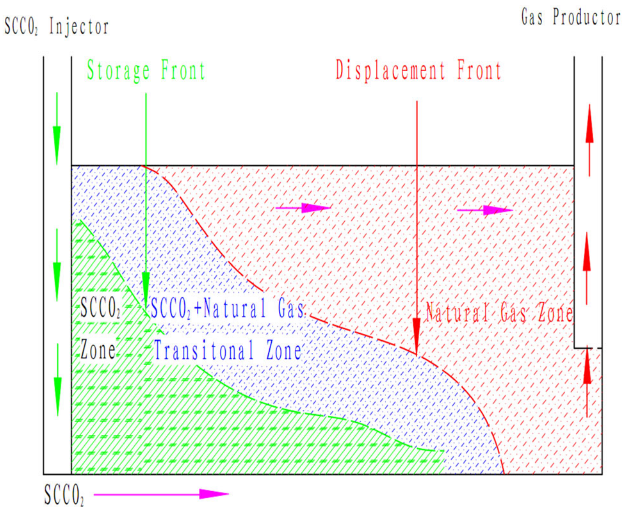

Fig. 1 Schematic of CSEGR in the horizontal direction

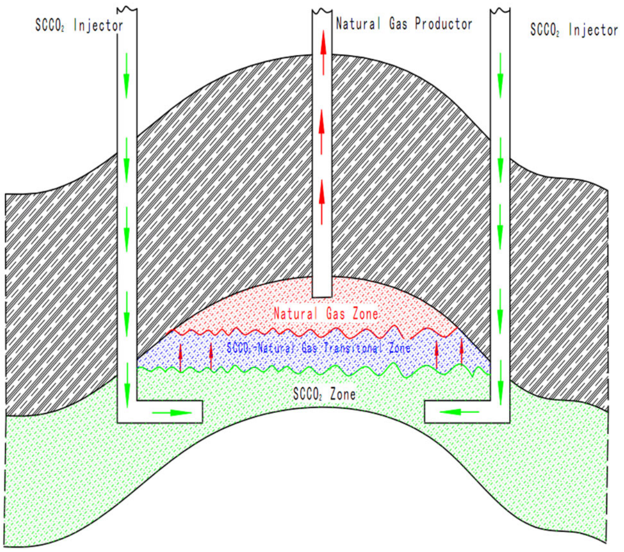

Fig. 2 Schematic of CSEGR in the vertical direction

Some researchers now believe that gas condensate reservoirs are another possible site for CCS because the rise in formation pressure caused by a $SCCO_2$ injection can enhance condensate oil recovery (Sobers et al. 2004; Mbarrufet et al. 2009; Ramharack et al. 2010). That condition requires more $SCCO_2$ to mix with the condensate gas, which is very different from the CSEGR method discussed in this paper.

There are still other studies in the literature by famous research groups that delve into coupling oil recovery and carbon sequestration, such as “Micromodel investigations of CO_2 exsolution from carbonated water in sedimentary rocks” (Zuo et al. 2013), “Multi-scale experimental study of carbonated water injection” (Alizadeh et al. 2014), “CO_2 injection as an immiscible application for enhanced recovery in heavy oil reservoirs” (Khatib et al. 1981) and so on.

In this paper, the sequestration site is a PY gas reservoir. The pressure, volume and temperature (PVT) properties of the $SCCO_2$ zone, $SCCO_2$–natural gas transitional zone and natural gas zone are tested by experiments or calculated by a program based on the PR-EOS, using *Z*-factor, Volume ratio in place ($V_{r.scco_2}$), density and viscosity. We discuss those results to understand the phase behavior of each fluid zone during the gases migrations in gas reservoirs under the repressurization caused by the active CO_2 injection. We also attempt to assess the ideal injection site and several eligible pressures for CSEGR based on such PVT properties. The paper makes clear the necessity and feasibility of CO_2 sequestration in reservoirs and CO_2 injection for the improvement of gas recovery. It accordingly recommends the feasible injection depth of supercritical CO_2 and the practical gas production pressure range for enhancing the recovery of the PY gas reservoir.

Theory

Z-factor

CSEGR depends on the supercritical phase behavior of CO_2 and the multi-contact between $SCCO_2$ and the natural gas. The degree of nonideality and supercriticality shown by the gases can be expressed by the *Z*-factor. *Z*-factor is also the key to gain other PVT properties. We have generated *Z*-factors for the $SCCO_2$ zone, $SCCO_2$–natural gas transitional zone and natural gas zone of the target gas reservoir by experimental and phase calculation methods.

Laboratory measurements are taken with the use of a PVT cell. The basic operation consists of pressurizing a known volume of gas in a PVT cell within a temperature-controlled oven (Sobers et al. 2004). In this paper, the *Z*-factors of pure CO_2, a 23.33 % CO_2–natural gas mixture and the pure natural gas are determined by experimental testing. Such *Z*-factors are tested by the DBR company’s JEFFRI PVT instrument, which can be used under high temperatures and pressures. When Z_f is defined as the *Z*-factor for PVT cell conditions, the experimental testing method is given by:

$$Z_f = \frac{V_f P_f T_{sc}}{V_{sc} T_f P_{sc}} \quad (1)$$

where V_{sc} (m^3) is the gas volume at standard temperature, T_{sc} (°C), and standard pressure, P_{sc} (Pa). V_f is the gas volume at the temperature and pressure in the PVT cell. Z_f is the *Z*-factor under cell PVT conditions. The standard condition in China is 20 °C and 1.10e5 MPa.

Then, we select the suitable calculation method for the *Z*-factor based on the measured values for a 23.33 % CO_2 (volume fraction)–natural gas mixture under different conditions. The calculation method options are the Soave–Redlich–Kwong EOS (Soave 1972), Peng–Robinson EOS (Peng and Robinson 1976) and experience formulas such as the Hall–Yarborough method (Hall and Yarborough 1973), Dranchuk–Purvis–Robinson method (Dranchuk et al. 1974), Dranchuk–Abu–Kassem method (Dranchuk and Abou-Kassem 1975), Hankinson–Thomas–Phillips method (Hankinson et al. 1969), Li method (Li and Gang 2001) and Zhang method (Zhang et al. 2005). Experience formulas need to be combined with non-hydrocarbon correction methods to gain the higher accuracy of the acid gas prediction. We choose the Guo correction (Guo et al. 2000). The PR-EOS has the greatest accuracy and fits with the Chinese oil/gas engineering standard to predict the *Z*-factors of a CO_2–natural gas mixture. The relative average deviation for different conditions is 0.94 %. Therefore, we select the PR-EOS to predict the *Z*-factors of the formation fluid.

Volume ratio in the place ($V_{\mathrm{r.scco_2}}$)

CSEGR, as a development of CCS, should also account for the effect of carbon sequestration. To do this, the Volume ratio in place ($V_{\mathrm{r.scco_2}}$) as the volume ratio between the formation fluid and CO_2 of the same moles on a certain reservoir condition is defined. If this parameter is less than 1, the volume of the formation fluid is less than the same moles of CO_2. Such a condition will be helpful to CO_2 storage. On the other hand, if this parameter is greater than 1, the fluid squeezes the $SCCO_2$ storage space and is more useful to EGR than $SCCO_2$ under the formation conditions. The Volume ratio in place ($V_{\mathrm{r.scco_2}}$) is given by:

$$V_{\mathrm{r.scco_2}} = \frac{V_i}{V_{\mathrm{CO_2}}} = \frac{Z_i T_i P_{\mathrm{f}}}{Z_{\mathrm{CO_2}} P_i T_{\mathrm{f}}} \tag{2}$$

where $V_{\mathrm{r.scco_2}}$ is the Volume ratio in place, V_i (m^3) is the gas volume at a certain temperature, T_i (°C), and certain pressure, P_i (Pa), and Z_i is the *Z*-factor under the same conditions. "*i*" can be the pure CO_2 at another temperature or pressure. The $V_{\mathrm{r.scco_2}}$ can be helpful to estimate the ideal injection site for CO_2. "*i*" can be the CO_2–natural gas mixture, or the natural gas. Then, the $V_{\mathrm{r.scco_2}}$ suggests the ability of EGR with $SCCO_2$. $V_{\mathrm{CO_2}}$ (m^3) is the volume of the pure CO_2 system under certain reservoir conditions, and $Z_{\mathrm{CO_2}}$ is the *Z*-factor for such conditions.

We can plot the $V_{\mathrm{r.scco_2}}$–pressure ($V_{\mathrm{r.scco_2}}$–p) curves of the $SCCO_2$ zone, $SCCO_2$–natural gas transitional zone and natural gas zone of the target gas reservoir by Eq. (2) based on *Z*-factors.

Density and viscosity

Density and viscosity are important PVT properties affecting the gases migrations in the reservoir. However, traditional experiments for these two-phase properties are usually costly or time-consuming. Many experts used novel correlations to study the density and viscosity in PVT experiments. Hemmati-Sarapardeh et al. (2013) studied reservoir oil viscosity correlations. Naseri et al. (2014) found a correlation approach for predicting the PVT properties of reservoir oils. We have made a program mainly based on the PR-EOS to predict viscosity and density together, and the viscosity model of a program presented by Guo (Guo et al. 1999) and based on the PR-EOS. Compared with the two above predictions, the calculated results are credible and within the acceptable range.

The benefits of CSEGR

Target reservoir and the natural gas

PY gas reservoirs are located in the high point of the TYY structure of EHD fault-salient in a LC rifted basin (Fig. 3). Its depth is 900–1028 m. Geological properties and the natural gas hydrocarbon composition of the TQ layer are shown in Table 1. It is estimated as a low permeability and low porosity reservoir with low dry gas reserves abundance. In addition, the reservoir has a tight cap rock without bulk porosity and bulk permeability above it (Fig. 4). It is a possible site to perform CSEGR.

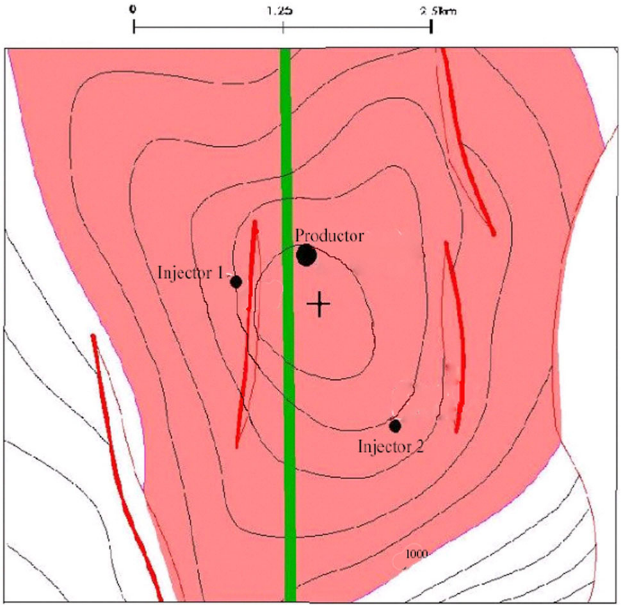

Fig. 3 PY arch structure reservoir

Table 1 Reservoir properties and natural gas composition of the QT layer

Geologic position	QT	Components	Mol%
Reservoir properties of QT layer		*The hydrocarbon groups of QT natural gas*	
Cover depth (m)	900–1028	CO_2	0.04
Precipitation facies	Fluvial deposition	N_2	5.7297
Lithology	Sandstone	C_1	92.6067
Neutron porosity (%)	5.17–12.57	C_2	1.4015
Bulk porosity (%)	10.0	C_3	0.0130
Bulk permeability (10^{-3} μm^2)	0.4–13.4	IC_4	0.0117
Mean permeability (10^{-3} μm^2)	6.0	NC_4	0.1825
Temperature gradients[a] (°C/100)	2.2	IC_5	0.0039
Hydrostatic pressure gradient (Mpa/100 m)	1.0	NC_5	0.0026
Formation pressure coefficient	1	FC_6	0.0091

[a] The standard condition in China is 20 °C, 0.110 MPa

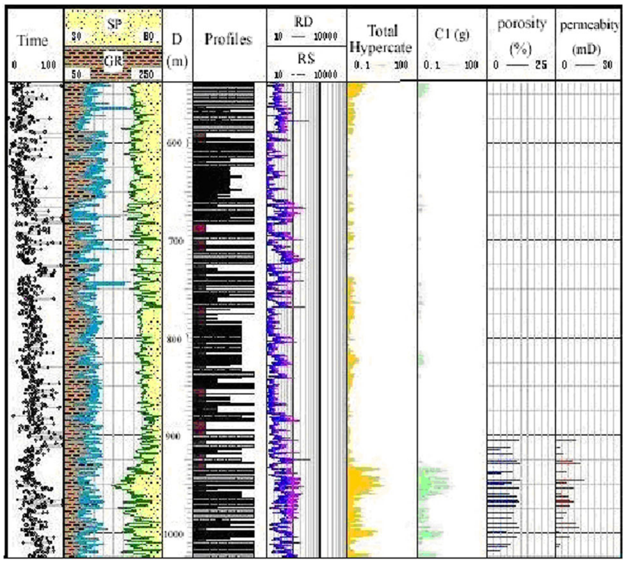

Fig. 4 Gas diagram of the PY

Phase behavior of natural gas

Figure 5 graphs the *Z*-factors–pressure (*Z*-factors–*p*) curves for natural gas. Figure 6 graphs the $V_{\mathrm{r.scco_2}}$–p curves of the gas in the TQ layer. Figure 7 graphs the phase diagram for the gas with iso-density lines. Moreover, Fig. 8 graphs the phase diagram for the gas with iso-viscosity curves. These figures have a typical pressure–temperature profile from the wellhead to the bottom of PY reservoir (*p*–*T* profile). Figure 5 suggests that the gas shows nearly ideal gas behavior and supercriticality is not obvious. Figure 6 indicates that the volume of the gas is over 2 times that of $SCCO_2$ in the reservoir. Figure 7 shows that the density of the gas is less than 100 kg/m^3. Figure 8 indicates that the

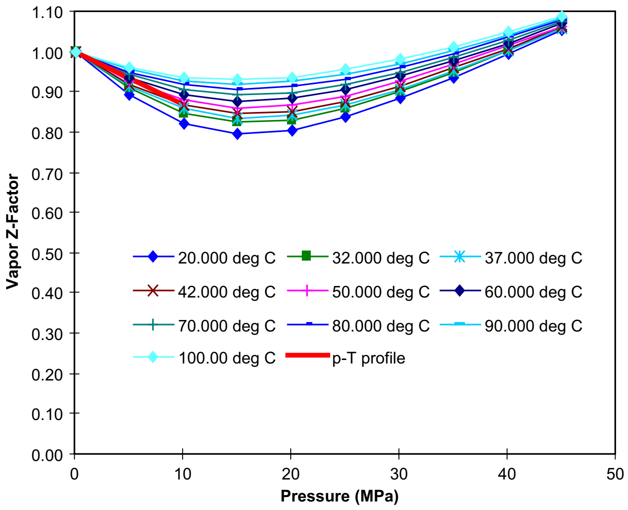

Fig. 5 *Z*-factors of natural gas

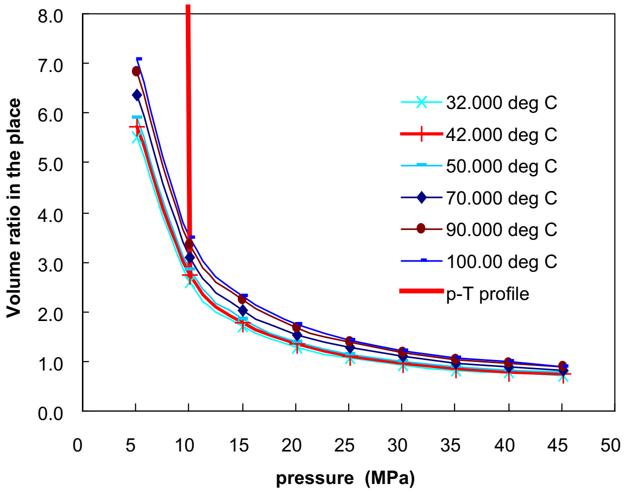

Fig. 6 Volume ratio in place ($V_{\mathrm{r.scco_2}}$) of natural gas

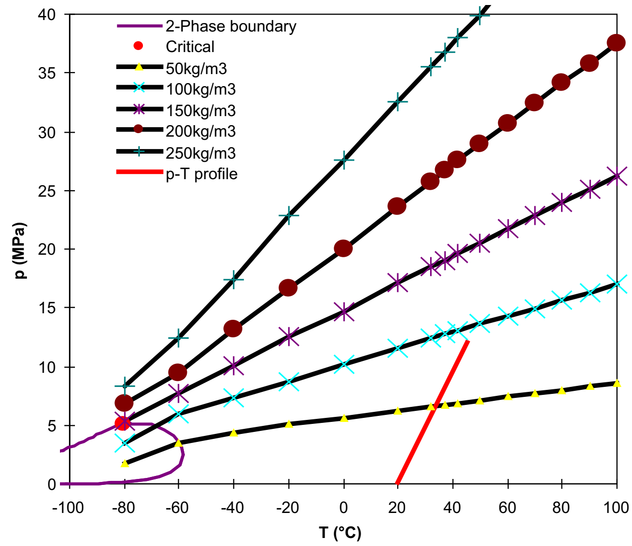

Fig. 7 Phase diagram of natural gas with iso-density lines

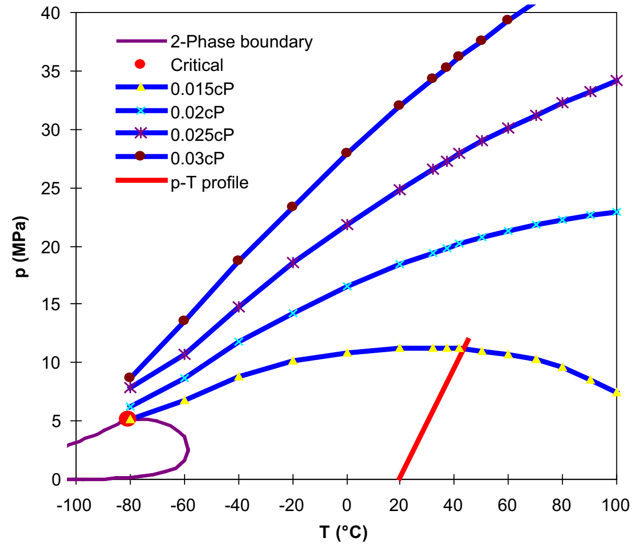

Fig. 8 Phase diagram of natural gas with iso-viscosity curves

viscosity of the gas is almost 0.01 cp under the reservoir conditions. The natural gas is light and thin.

The necessity of ESEGR in PY gas reservoir

Figures 5 and 6 suggest that natural gas will take up the pore space of reservoir, reducing the potential space of $SCCO_2$ storage. Thus, effective carbon storage in a PY gas reservoir should be combined with the production of the gas. It is not only good for the stable sequestration of the $SCCO_2$, but also the repressurization caused by active CO_2 injection will enhance natural gas recovery.

$SCCO_2$ zone and the ideal injection site

Phase behavior of $SCCO_2$ zone

Shown in Fig. 9 are the *Z*-factors of pure CO_2. Figure 10 is the $V_{\mathrm{r.scco_2}}$–p curves of pure CO_2. Figure 11 graphs the phase diagram for CO_2 with iso-density lines. Moreover, Fig. 12 graphs the phase diagram for CO_2 with iso-viscosity curves. Figure 9 indicates that the supercriticality of $SCCO_2$ is obvious for reservoir conditions. Figure 10 shows that the underground volume of $SCCO_2$ will self-contract quickly and then remain constant during an ongoing CO_2 injection. Figure 11 shows that the density of $SCCO_2$ will increase by 100 kg/m^3 under a 1–2 MPa pressure increase if the temperature is near the critical temperature. Figure 12 indicates that the viscosity of $SCCO_2$ is at the level of the gases and higher than the natural gas viscosity.

The ideal injected site

The ideal injection site of CSEGR must have the right depth with the right temperature to keep CO_2 in a supercritical state. Figures 9 and 10 suggest that a too high formation temperature should prevent the self-contraction of $SCCO_2$ for a maximum storage capacity in place. So deep gas reservoirs are not suitable for CSEGR. When $32\ ^\circ\mathrm{C} < T < 50\ ^\circ\mathrm{C}$ and $7.4\ \mathrm{MPa} < p < 20\ \mathrm{MPa}$, *Z*-factor–$p$ curves sag down acutely, and $V_{\mathrm{r.scco_2}}$ quickly decreases to 1. The density (over 600 kg/m^3, Fig. 11) is heavy enough to allow for CO_2 to migrate to the lower part of the reservoir. Based on such data, we believe 1000 m below (42 °C, 10 MPa; the relevant data are in Table 1.) the PY gas reservoir is available to both the effective $SCCO_2$ sequestration and CSEGR.

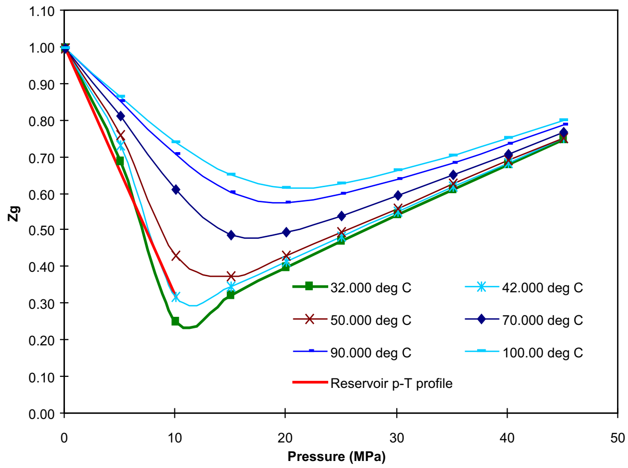

Fig. 9 Experimental *Z*-factors of pure CO_2

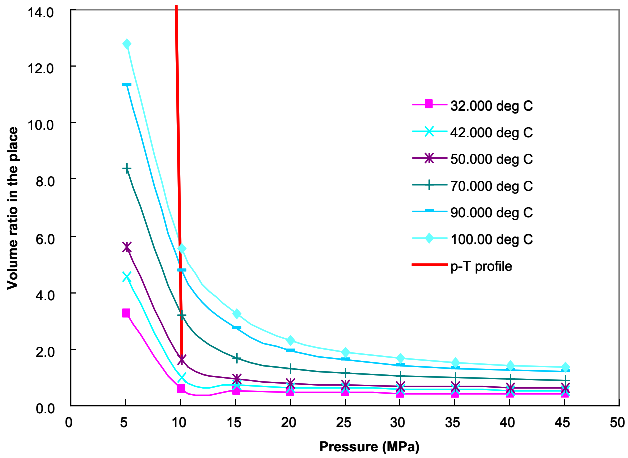

Fig. 10 $V_{\mathrm{r.scco_2}}$ of pure CO_2

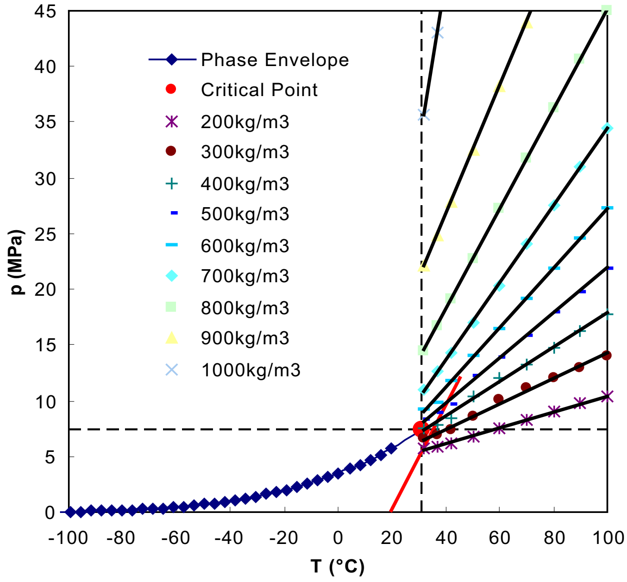

Fig. 11 Phase diagram of CO_2 with iso-density lines

$SCCO_2$–natural gas transitional zone and the suitable pressures

The multi-contact mix during the gas migration makes the natural gas concentration (Cn.g) decrease successively from the displacement front to the storage front. The phase properties of $SCCO_2$–natural gas mixtures with different Cn.g can reveal the supercriticality of the $SCCO_2$–natural gas transitional zone.

Phase behavior of $SCCO_2$–natural gas transitional zone

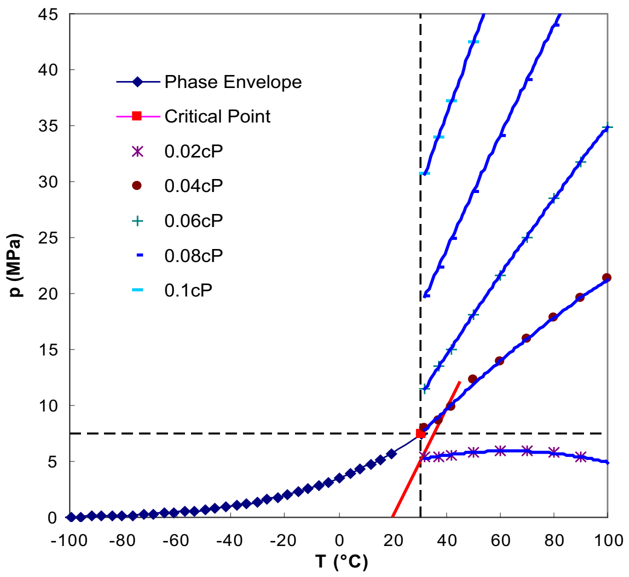

Fig. 12 Phase diagram of CO_2 with iso-viscosity curves

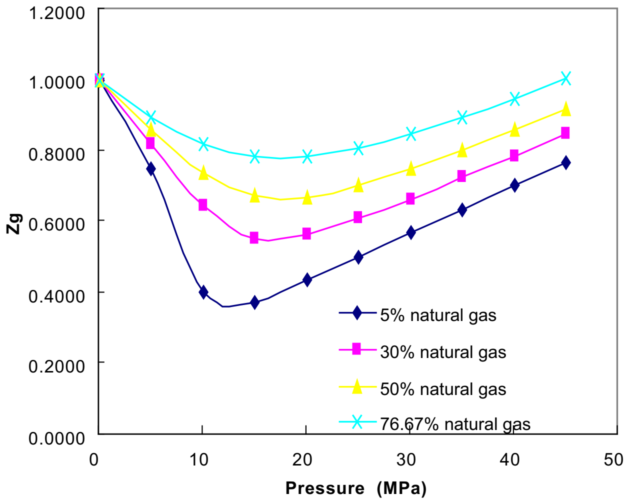

Fig. 13 Z–p profiles of the $SCCO_2$–natural gas transitional zone

Figure 13 graphs the Z-factor–p curves for the 4 Cn.g profiles (5, 30, 50 and 76.67 %) of the $SCCO_2$–natural gas transitional zone under the ideal $SCCO_2$ injection site temperature. Figure 14 shows the Z-factor–Cn.g curves. Figure 15 is the $V_{\mathrm{r.scco_2}}$–p curves. Figure 16 shows the density–Cn.g curves under reservoir conditions. Moreover, Fig. 17 shows the viscosity–Cn.g curves under reservoir conditions. Figures 14, 15, 16 and 17 demonstrate that the diffusion of the gas will weaken the supercriticality of the $SCCO_2$–natural gas transitional zone. In addition, supercriticality decreases from the storage front to the displacement front, while the $V_{\mathrm{r.scco_2}}$ increases. This demonstrates that the $SCCO_2$–natural gas transition zone is a "mechanical spring" in the natural gas zone, protecting the $SCCO_2$ storage space in the storage front and allowing for continuous CO_2 injection. At 10, 15 and 20 MPa, phase properties change faster than other pressures. It indicates

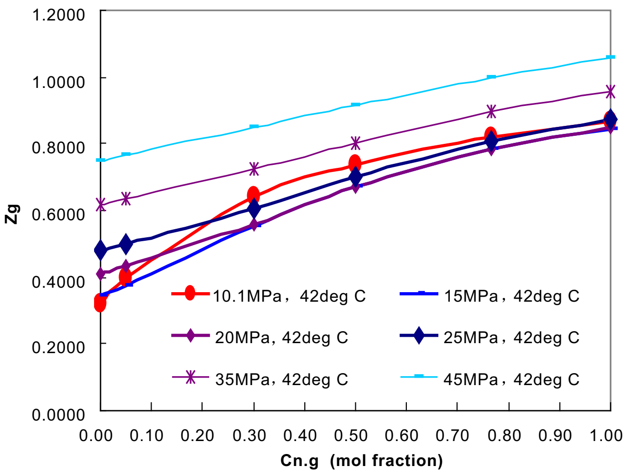

Fig. 14 *Z*–Cn.g curves of the $SCCO_2$–natural gas transitional zone

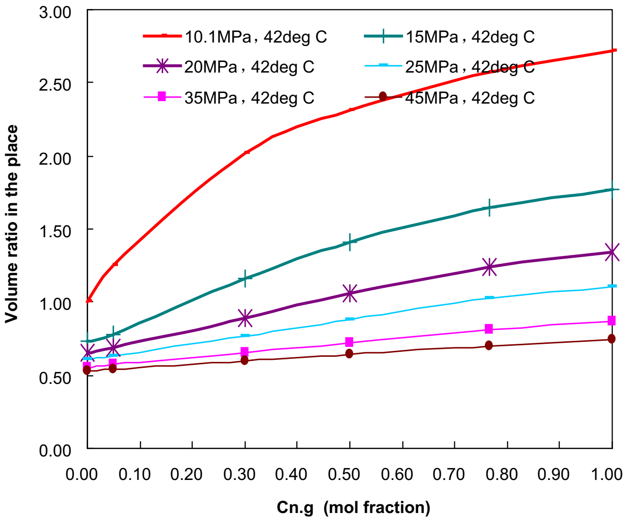

Fig. 15 The $V_{\mathrm{r.scco_2}}$ –Cn.g curves of the $SCCO_2$–natural gas transitional zone

that supercriticality is outstanding in such a pressure region.

The eligibly pressures

Assessing the feasible pressure of CSEGR in the field involves considering many controlling factors. However, we can obtain the eligible pressures for the next core-flooding test based on phase behavior research. This involves repressurization by continuous CO_2 injection to squeeze all fluid zones and the volume that the $SCCO_2$ zone can decrease to most quickly to maintain safe CO_2 storage. For ESEGR, the average $V_{\mathrm{r.scco_2}}$ of the $SCCO_2$–natural gas transition zone and the displacement front should be greater than 1 for EGR. In addition, the $V_{\mathrm{r.scco_2}}$ of the storage front should be less than 1 to protect the $SCCO_2$ zone and $SCCO_2$ storage.

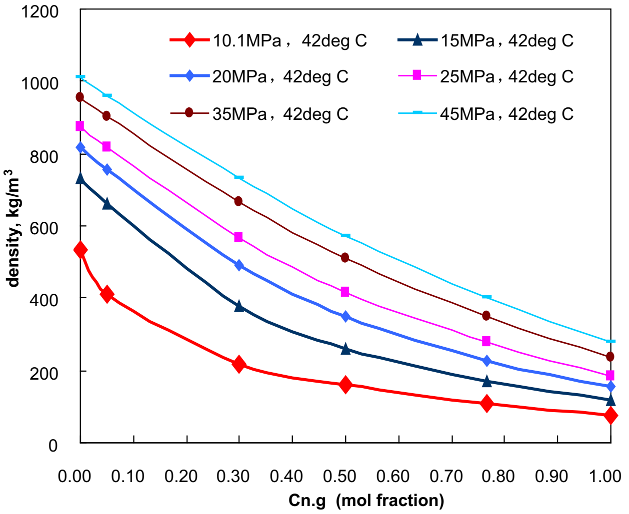

Fig. 16 Density–Cn.g curves of the $SCCO_2$–natural gas transitional zone

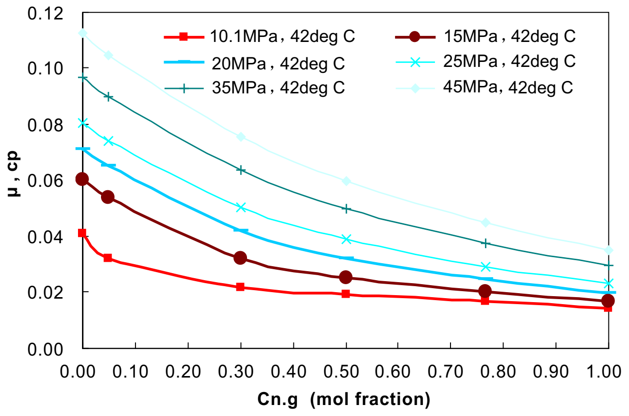

Fig. 17 Viscosity–Cn.g curves of the $SCCO_2$–natural gas transitional zone

We propose 3 schemes for CSEGR in the PY gas reservoir to estimate several eligible pressures. Scheme 1 is producing gas and keeping the ideal injection site pressure (10 MPa) by continuous $SCCO_2$ injection. Scheme 2 raises the formation pressure to 15 MPa. Moreover, Scheme 3 increases the formation pressure to 20 MPa. Table 2 lists the different $V_{\mathrm{r.scco_2}}$ for the schemes' $SCCO_2$–natural gas transitional zones. In Table 2, the average $V_{\mathrm{r.scco_2}}$ of the transitional zone and displacement front of both scheme 1 and scheme 2 are greater than 1. This suggests that transitional zones under 10 and 15 MPa would benefit from EGR. However, the $V_{\mathrm{r.scco_2}}$ of the storage front at these pressures is less than 1. This suggests that the transitional zones under 10 and 15 MPa would benefit from CO_2 storage in storage front and EGR in the displacement front. As the average $V_{\mathrm{r.scco_2}}$ is less than 1 in scheme 3, it suggests that transitional zones under 20 MPa only benefit from CO_2 sequestration. Therefore, scheme 1 and

Table 2 Volume ratio in place ($V_{r.scco_2}$) of the transitional zone at 10, 15 and 10 MPa

Cn.g profiles of transitional zone	$V_{r.scco_2}$ (10.1 MPa, 42 °C)	$V_{r.scco_2}$ (15 MPa, 42 °C)	$V_{r.scco_2}$ (20 MPa, 42 °C)
Storage front	1.00	0.73	0.65
0.05	1.25	0.78	0.68
0.3	2.01	1.16	0.89
0.5	2.32	1.41	1.06
0.7667	2.57	1.64	1.24
Displacement front	2.72	1.77	1.34
AVG	1.98	1.25	0.98

scheme 2 are the eligible schemes for CSEGR in a PY reservoir.

Conclusion

Natural gas will take up the pore space of a reservoir and reduce the potential space for $SCCO_2$ sequestration. Therefore, CSEGR is necessary if we conduct CO_2 sequestration in a PY gas reservoir. Multi-contact during the gas migration in CSEGR forms the $SCCO_2$–natural gas transitional zone. Thus, the formation fluid in the whole reservoir could be simply divided into three zones on the swept region. Such areas are the $SCCO_2$ zone, $SCCO_2$–natural gas transitional zone and natural gas zone. The PVT properties of the formation fluid may be summarized as follows:

An ideal CO_2 injection place is significant to the ideal gases migration during CSEGR. The ideal CO_2 injection site should have the right temperature to keep the gravitational differentiation between the $SCCO_2$ and natural gas large enough. In addition, the $SCCO_2$ zone should be at a stable volume for $SCCO_2$ storage. Thus, the $SCCO_2$ zone will stay in the lower part of reservoir. The natural gas zone will rise to the higher part of reservoir for gas production. The $SCCO_2$–natural gas transitional zone can separate the other two fluid zones into certain regions. Thousand meters beneath the PY gas reservoir is available to both effective $SCCO_2$ sequestration and CSEGR.

Repressurization by continuous CO_2 injection squeezes all of the fluid zones. The volume of the $SCCO_2$ zone can decrease quickly to maintain safe CO_2 sequestration under a suitable pressure for CSEGR. Thus, the $SCCO_2$–natural gas transition zone should be more useful to EGR under a suitable pressure for CSEGR than $SCCO_2$ under original formation conditions. In addition, the transition zone is a "mechanical spring" in the natural gas zone, protecting the $SCCO_2$ storage space in the storage front and allowing for the continuous CO_2 injection. Based on phase behavior research, the ideal injection site pressure (10 MPa) and 15 MPa pressure are the eligible pressures for CSEGR in a PY reservoir.

Acknowledgments This research work was supported by the National Natural Science Foundation of China (51474180).

References

Alizadeh AH et al (2014) Multi-scale experimental study of carbonated water injection: an effective process for mobilization and recovery of trapped oil. Fuel 132:219–235

Blok K, Williams RH, Katofsky RE et al (1997) Hydrogen production from natural gas, storage of recovered CO_2 in depleted gas wells and enhanced gas recovery. Energy 22(2/3):161–168

Dranchuk PM, Abou-Kassem (1975) Calculation of Z-factors for natural gases using equations of state. JCPT 14(3):34–36

Dranchuk PM, Purvis RA, Robinson DB (1974) Computer calculations of natural gas compressibility factors using the standing and Katz correlation. Inst Pet Tech Ser 36(4):76–80

Guo XQ, Rong SX, Yang JT et al (1999) The viscosity model based on PR-EOS. Acta Pet Sin 20(3):56–61

Guo XQ, Yan W, Chen S et al (2000) Comparison of methods for calculating compressibility factor of natural gas at elevated high pressure. J Univ Pet (Nat Sci Ed) 24(6):36–39

Hall KR, Yarborough L (1973) A new equation-of-state for Z-factor calculations. Oil Gas J 37(8):82–92

Hankinson RW, Thomas LK, Phillips KA (1969) Predict natural gas properties. Hydrocarbon Process 48(4):106–108

Hemmati-Sarapardeh A et al (2013) Toward reservoir oil viscosity correlation. Chem Eng Sci 90:53–68

Khatib AK, Earlougher RC, Kantar K (1981) CO_2 injection as an immiscible application for enhanced recovery in heavy oil reservoirs. SPE California regional meeting. Society of Petroleum Engineers

Kubus P (2010) CCS and CO_2-storage possibilities in Hungary. SPE 139555 presented at the SPE international conference on CO_2

capture, storage, and utilization, New Orleans, LA, USA, 10–12 Nov 2010

Li XF, Gang T (2001) A analytic model with high precision for calculating compressibility factor of high-pressure gas. J Univ Pet (Nat Sci Ed) 25(6):45, 46, 51

Mamora DD, Seo JG (2002) Enhanced gas production by carbon dioxide storage in depleted gas reservoirs. Society of Petroleum Engineers, Paper SPE-77347 presented at the SPE annual technical conference and exhibition, San Antonio, TX, USA, 29 Sept–2 Oct 2002

Mbarrufet A, Bacquet A, Falcone G (2009) Analysis of the storage capacity for CO_2 storage of a depleted gas condensate reservoir and a saline aquifer. Paper 2009-197 presented at the Canadian international petroleum conference (CIPC) 2009, Calgary, AB, Canada, 16–18 June 2009

Naseri A et al (2014) A correlations approach for prediction of PVT properties of reservoir oils. Pet Sci Technol 32(17):2123–2136

Nogueira MC, Mamora DD (2005) Effect of flue gas impurities on the process of injection and storage of CO_2 in depleted gas reservoirs SPE-94906-STU (Student 19) presented at the 2005 SPE/EPA/DOE exploration and production environmental conference, Galveston, TX, USA, 7–9 Mar 2005

Oldenburg CM (2003) Carbon storage in natural gas reservoirs: enhanced gas recovery and natural gas storage. In: Tough symposium proceedings, pp 1–8

Peng DY, Robinson DB (1976) A new two-constant equation of state. Ind Eng Chem 15(1):59

Ramharack R, Aminian K, Ameri S (2010) Impact of carbon dioxide storage in gas/condensate reservoirs. SPE 139083 presented at the SPE eastern regional meeting, Morgantown, WV, USA, 12–14 Oct 2010

Seo JG, Mamora DD (2003) Experimental and simulation studies of storage of supercritical carbon dioxide in depleted gas reservoirs. Paper SPE 81200 presented at the SPE/EPA/DOE exploration and production environmental conference, San Antonio, TX, USA, 10–12 Mar 2003

Soave G (1972) Equilibrium constants from a modified Redlich–Kwong equation of state. Chem Eng Sci 27(6):1197

Sobers LE, Frailey SM, Lawal AS (2004) Geological storage of carbon dioxide in depleted gas reservoirs. SPE 89345 presented at the 2004 SPE/DOE fourteenth symposium on improved oil recovery, Tulsa, Oklahoma, USA, 17–21 Apr 2004

Turta AT, Sim SSK, Singhal AK et al (2008) Basic investigations on enhanced gas recovery by gas–gas displacement. J Can Pet Technol 47(10):39–44

Van der Meer LGH, Kreft E, Geel C et al (2005) K12-BA test site for CO_2 storage and enhanced gas recovery. Paper SPE 94128 presented at the SPE Europec/EAGE annual conference, Madrid, Spain, 13–16 June 2005

Zhang GD, Li M, Bai DL (2005) Practical calculating model of gas deviation factor with high and super-high pressure 1. Nat Gas Ind 25(8):79, 80, 93

Zuo L et al (2013) Micromodel investigations of CO_2 exsolution from carbonated water in sedimentary rocks. Adv Water Resour 53:188–197